COVER FEATURE BETTER LIVING THROUGH CHALLENGES



Shane Allcroft[®], Mohammed Metwaly, Zachery Berg[®], Isha Ghodgaonkar, Fischer Bordwell¹⁰, XinXin Zhao, Xinglei Liu¹⁰, and Jiahao Xu, Purdue University Subhankar Chakraborty, Indian Institute of Technology Madras Vishnu Banna, Akhil Chinnakotla[®], Abhinav Goel[®], Caleb Tung[®], Gore Kao, and Wei Zakharov, Purdue University David A. Shoham, East Tennessee State University George K. Thiruvathukal¹⁰, Loyola University Chicago Yung-Hsiang Lu[®], Purdue University

This article analyzes visual data captured from five countries and three U.S. states to evaluate the effectiveness of lockdown policies for reducing the spread of COVID-19. The main challenge is the scale: nearly six million images are analyzed to observe how people respond to the policy changes.

n 11 November 2019, the first known case of the novel coronavirus, SARS-CoV-2 (COVID-19), was reported. On 14 January 2020, the World Health Organization warned that the fast-spreading virus could become cross-national. 2 By March 2020, COVID-19 had spread across the globe, and the disease was officially considered a pandemic.3 Since then, countries implemented lockdown policies intended to limit mobility (the amount of a population that is in a public space) and the formation of human clusters, both of which contribute to the spread of the disease in epidemiology models.

UNDERSTANDING THE REACTIONS TO LOCKDOWN POLICIES

Understanding people's responses to lockdown policies is important for evaluating the effectiveness of the policy and making adjustments. However, gathering meaningful data about people's mobility over time is challenging. Any form of in-person observation would risk infection of the observers, introduce observation bias, and generally be infeasible to sustain consistently for a long time period.

The current automated solutions for gathering data describing mobility are limited in the following ways. First, automated attempts to quantify mobility as it relates to public activity started on a large scale only in 2020. While the COVID-19 pandemic has spurred advancements in mobility research, current data collection methods are usually based on voluntary opt-in via mobile phone networks. These methods introduce collection bias and limit the ability to generalize to the entire population. Second, tracking mobile phone users raises questions about

privacy. Third, the evaluation method should consider the responses of the general public, not specific individuals of mobile phone users.

This article presents a method to observe mobility over time at a global scale using computer vision applied to the data captured by network cameras. Through the camera discovery method previously developed by this team, 4 we discover 30,254 existing public network cameras. The list of cameras is reduced to 17,795 by applying an image scene archetype classifier to exclude data from cameras unlikely to see people or vehicles. The list is further reduced to 3,469 cameras from five countries (Australia, Austria, France, Germany, and Italy) and three U.S. states (Georgia, Oregon, and Hawaii) with distinct lockdown policies. The analysis method detects people and vehicles from 1 April 2020 to 8 March 2021 (334 days).

This study counts the number of people and vehicles in nearly six million images. The analysis is able to observe meaningful mobility trends and relative mobility levels with a resolution down to a single day. The observed mobility trends reflect specific policy changes in each region. This article compares these trends of mobility in relation to the Oxford Stringency Index⁵; this index measures governments' responses to COVID-19. The observed mobility trends demonstrate that this method has the potential for understanding how people will respond to policies in future pandemics.

RELATED WORK

Before the COVID-19 pandemic, there were few methods for the quantification of mobility. Since then, efforts have been made to quantify mobility using mobile phone data. Google⁶ collects data from smartphone users who

have opted into sharing their location history and aggregates those data into "movement trends over time." Apple reports mobility through the number of Apple Maps requests for directions made in a given geographical region, categorizing requests into three categories of walking, driving, and using public transit. Both reports anonymize the data they collect.

A web application⁸ allows users to compare data from Apple's Mobility Trends Reports, confirmed numbers of COVID-19 cases, and government response policies for a particular country or U.S. state or county. Pedestron⁹ is a popular repository for person detection for counting the number of people in images. Computer vision can classify images into archetypes. CSAIL-Places 365¹⁰ is an image data set with 365 scene categories, such as highway, crosswalk, and restaurant. CrowdHuman¹¹ is a data set and can be used to train neural network models (such as Cascade R-CNN^{12,13}) to count the number of people in an image. The MS COCO data set¹⁴ contains different types of vehicles, such as cars, trucks, motorcycles, and buses.

HOW WE OBSERVE MOBILITY

This article uses the visual data (images and video) from network cameras to observe human mobility over time. The mobility is measured by the number of people or vehicles in public locations. Figure 1 shows three examples of network cameras. Network cameras capture visual data and transmit the data over the Internet. This study uses only public data; the data are available to anyone that is connected to the Internet, without any password protection. This study discovers network cameras worldwide and then selects the cameras that are



FIGURE 1. Three snapshots captured on different days from three locations. We counted the people in each image by hand and found 33, 85, and 70 people in each image, respectively. Pedestron found 31, 84, and 68 people, respectively. The right images show correctly detected bounding boxes containing people (green), false positives (red), and false negatives (blue). (a) Aydat, France, 11 August 2020. (Source: www.meteosurfcanarias.com.) (b) Kerns, Switzerland, 29 December 2020. (Source: Snoweye.com.) (c) Žatec, Czech Republic, 15 May 2020. (Source: webcam.mesto-zatec.cz.)

likely to see humans or vehicles. This study captures data regularly from these selected cameras between April 2020 and March 2021. The numbers of humans and vehicles are compared over time as well as the Oxford Stringency. This analysis suggests that the visual data can be an effective method for quantifying people's responses to the lockdown policies. Figure 2 shows the flow of this study.

Discover and select network cameras

The first step of this study is to discover network cameras. Many organizations (such as departments of transportation and national parks) and individuals deploy network cameras and make the data available on the Internet. This team has created an Internet crawler that can discover visual data this crawler captures multiple snapshots from each camera to determine whether the visual data change over time. This method discovers 30,254 cameras deployed in different parts of the world; three examples are shown

in Figure 1. Between April 2020 and March 2021, five snapshots were taken per day from each camera to estimate the number of people and vehicles. The locations of the cameras can be determined using several methods. Many cameras are deployed by departments of transportation, and the locations are marked by the owners. This study further validates the locations using Google Street View/Google Earth data found at the latitude and longitude reported by the camera (see Figure 3).

Some of the discovered cameras do not provide insightful data for observing mobility trends. For instance, some cameras see mountains and cannot see people or vehicles. Some other cameras have very low refresh rates. Due to the large number of discovered cameras, this study uses automated methods to select the discovered cameras. The first step is to eliminate the cameras whose data do not refresh frequently. This study captures five snapshots from each camera per day; thus, this step keeps only the 23,291 cameras that refresh at least five times

per day. The second step uses the Wide Resnet18 model trained on the CSAIL-Places365 data set to determine the scene archetypes of the cameras and selects the scenes that likely observe people or vehicles, such as "park," "crosswalk," "highway," or "road." This process keeps 17,795 cameras, including 2,077 for observing people, 13,808 for observing vehicles, and 1,910 for both. The third step considers the regions where lockdown policies have been announced and adjusted over time and identifies the regions with multiple cameras. Finally, 3,469 cameras are selected for this study.

Localize network cameras

To correlate the mobility trends observed from network cameras and the lockdown policies, knowing the cameras' locations is essential. Several methods are used to determine the cameras' locations. Many camera owners set up the cameras with location information. The information may be longitude/latitude, street intersections, marks on highways, or tourist attractions. This

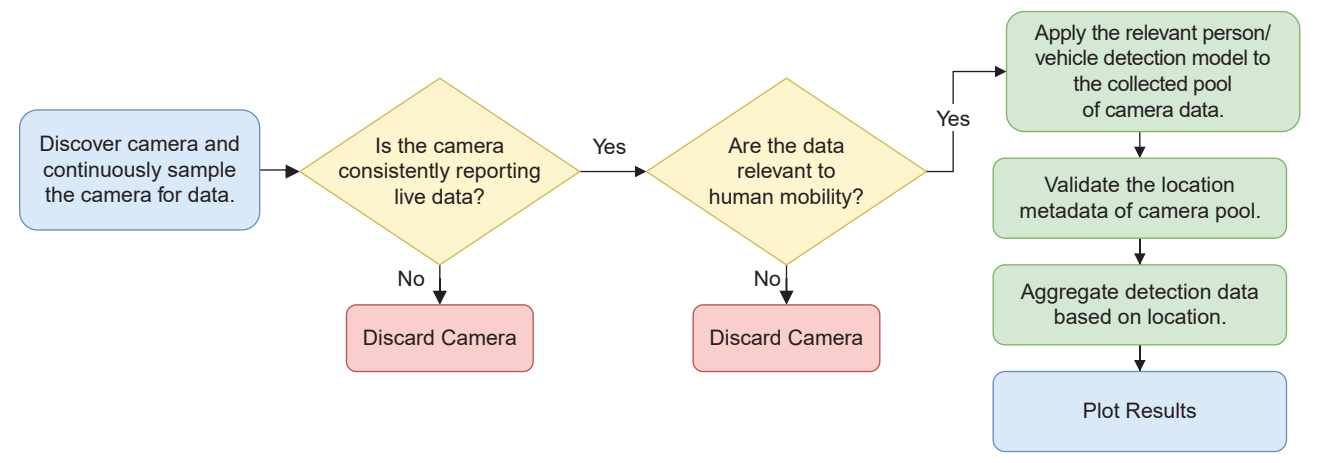


FIGURE 2. The workflow of the method presented in this article. The first step is to discover network cameras on the Internet. Some discovered cameras are discarded because they provide no meaningful data for quantifying human mobility (defined as seeing people or vehicles). Then, the numbers of observed people and vehicles are counted at the specific locations and time.

study validates the cameras' geographical locations using Google Earth and Google Street View where available. The study selects 100 cameras to validate the reported locations. Figure 3 shows an example. Figure 3(a) is an image from one discovered network camera; Figure 3(b) shows the image obtained from a Google Street View at the camera's reported location of (40.7514, -73.9934). The green circles indicate the displays seen in both images.

Collect and analyze data

From April 2020 to March 2021, this study uses cron in Linux running on a computer cluster with large-scale storage (in petabytes) for retrieving five images per camera each day, saving, and analyzing the data. Pedestron is used to count people; vehicles are detected using YOLOv3. Nearly six millionimages (fiveimages/camera-day × 3,469 cameras × 334 days = 5,793,230, 2.56 TB portable network graphics files) are analyzed. Due to the volume of the data, it is not possible to check the correctness of every image in the same way as Figure 1. If a person spent

1 min counting people or vehicles in each image, this person would spend 11 years. This is obviously impractical. Instead, this study uses 1,000 images as a validation data set to select the tuning parameters and to quantify the accuracy of the computer vision methods. These images are labeled manually with the correct counts; Figure 4 shows three examples in the validation data set.

Figure 5 shows the object detection F1 score (the metric we use to evaluate object detection model accuracy) with different confidence thresholds. When the threshold is low, too many false positives are detected. When the threshold is high, too many false negatives are neglected. The figure shows that 0.2 is a good value for both people and vehicle detection.

ANALYSIS OF MOBILITY TRENDS

This section presents the observed changes in mobility in five countries (Austria, Australia, France, Germany, and Italy) and three U.S. states (Hawaii, Georgia, and Oregon). These regions are selected because 1) they have specific policies, and these policies changed over time, and 2) sufficient numbers of cameras were discovered to observe different locations in each region. For the United States, different states have different policies, and they changed at different times.

Figure 6 summarizes the observed mobility changes. Each region is represented by three curves: the seven-day average of 1) the number of people, 2) the number of vehicles, and 3) the leniency of mobility restrictions. The third curve is obtained by taking the Oxford Stringency Index (a larger value means more restrictions) from each region and subtracting from the maximum possible stringency value (a larger value means fewer restrictions). Since our analysis is region wide, we do not include policies that are labeled as "targeted policies," which are policies targeting a subregion. This is referred to as the leniency index in this article. The markers in the figure indicate significant dates relating to the policy changes. These regions gradually lifted restrictions in the summer of 2020, indicated by the gradual rising of the





FIGURE 3. Validating a camera's location. (a) A snapshot from a discovered network camera. (b) Google Street View near the camera's reported location. (a) and (b) New York City, NY, USA, 1 August 2020. (Source: http://207.251.86.238/cctv19.jpg.)







FIGURE 4. (a)—(c) Three examples of images labeled by hand for our validation data set. Blue bounding boxes denote people, and red bounding boxes denote vehicles. (a) Dublin, Ireland, 8 June 2020. (Source: www.earthcam.com.) (b) Washington State, USA, 22 June 2020. (Source: dev.whidbeytel.com/cams/clinton/.) (c) Krakow, Poland, 23 June 2020. (Source: imageserver.webcamera.pl.)

indexes. The figure shows close correlations between the people and vehicle counts and the leniency index. When a region's policy changed (indicated by the leniency index), the mobility rose and declined accordingly.

The figure shows a dichotomy; the mobility in the first four regions

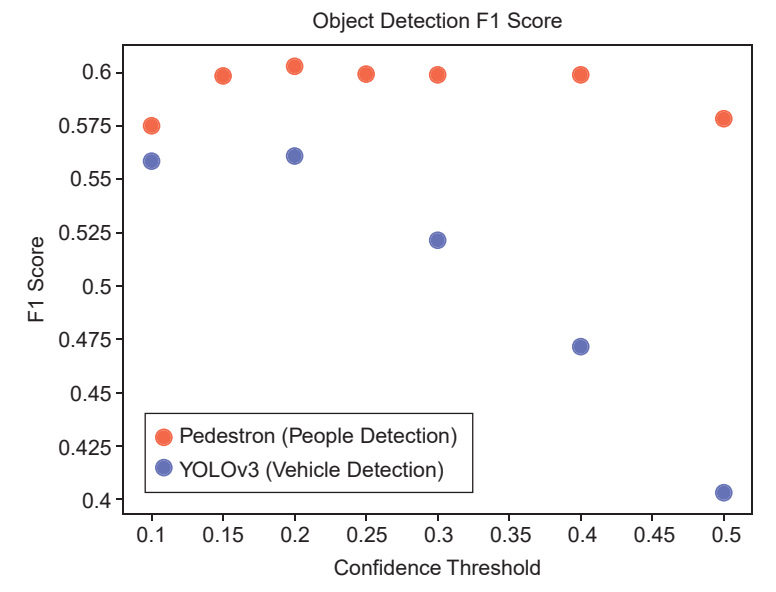


FIGURE 5. An F1 score plot for YOLOv3 (blue) and Pedestron (red) expressing how the F1 score on our validation data set varied when different values for the confidence hyperparameter were applied.

(France, Germany, Austria, and Italy) follows the index closely, but the other four regions (Australia, Hawaii, Georgia, and Oregon) do not show similar correlations. This can be explained by the different degrees of restrictions. The first four regions had extensive lockdowns, practically shutting down all businesses. The other four regions were less restrictive, resulting in much flatter leniency curves. The first four regions show noticeable changes in mobility, but the other four regions do not show similar patterns. Australia and Hawaii are two unique cases; they imposed travel restrictions for visitors, while the residents enjoyed relatively high degrees of freedom. There are small gaps in the data arising from supercomputer maintenance and rare occasions where jobs were not scheduled for up to one day. The missing data do not affect the observed trends.

To quantify the correlations between the people and vehicle counts and leniency index, we performed two Pearson correlation tests for each region:

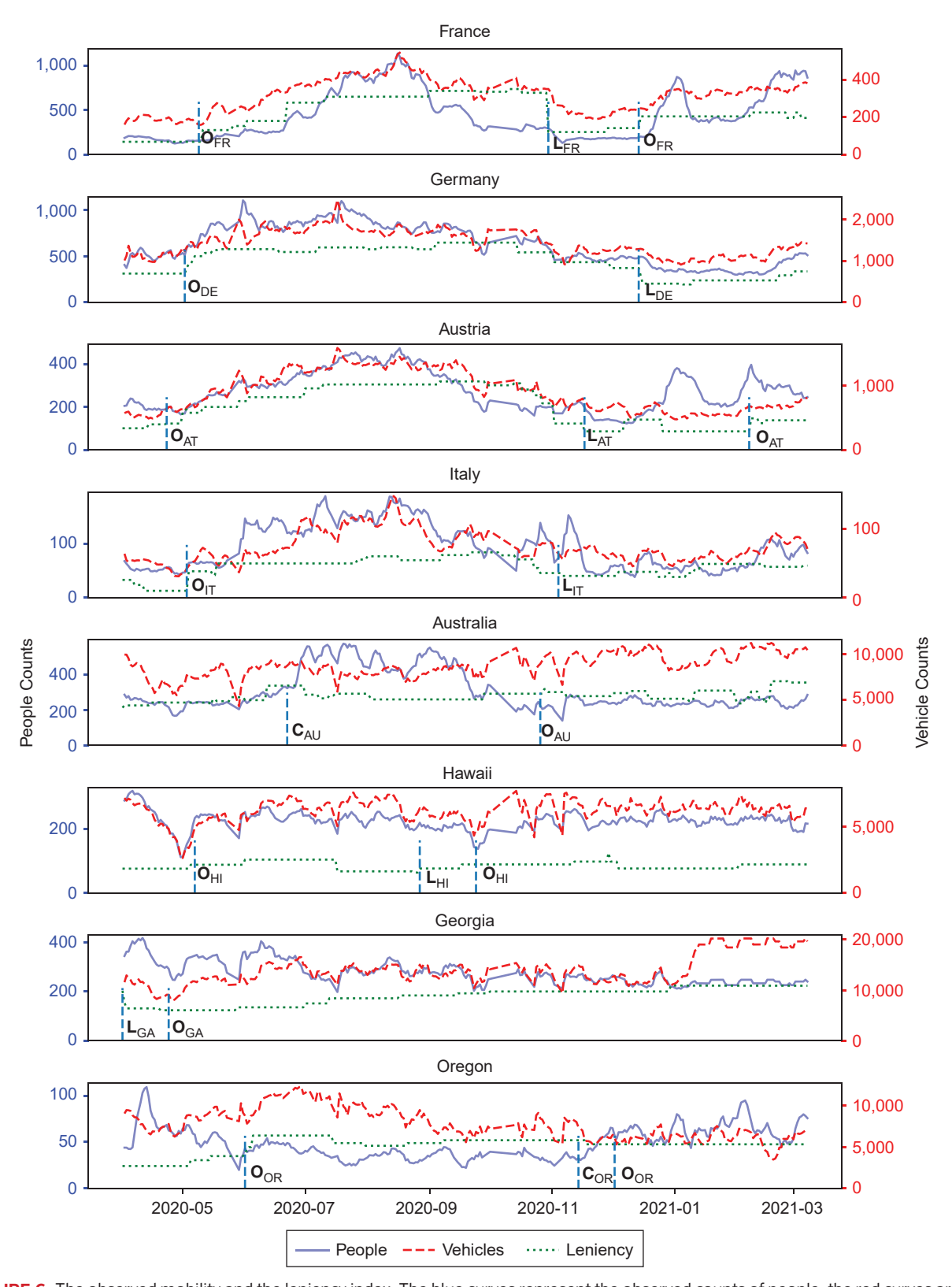


FIGURE 6. The observed mobility and the leniency index. The blue curves represent the observed counts of people; the red curves are the observed numbers of vehicles; and the green curves represent the restrictions (higher values mean fewer restrictions). Key policy dates are marked. The bold L represents a hard region-wide lockdown, the bold C represents government mandated closing of business or schools, and the bold O represents reopening, followed by higher values of the leniency index.

people detections versus the leniency index and vehicle detections versus the leniency index. The regions that exhibited strong positive correlation between observed mobility and the leniency index are France (people versus leniency = 0.5589, vehicles versus leniency = 0.7949); Germany (0.8140, 0.5328) (see also Figure 7); Austria (0.5106, 0.67); and Italy (0.5796, 0.6365). The regions that exhibited relatively weak correlation are Australia (-0.004, 0.2404); Hawaii (0.0236, -0.06); Georgia (-0.7516, 0.3966); and Oregon (-0.4348, 0.0469). Regions that exhibited a strong positive

correlation all had both Pearson coefficients (for people and vehicle versus leniency) average greater than +0.5, while the weakly correlated regions all had both Pearson coefficients average between -0.25 and +0.25.

When examining the policies of these two groups, we can see that the aforementioned dichotomy is reinforced by the raw numbers as well. The regions with high levels of correlation between observed mobility and leniency all have a policy timeline characterized by hard "stay at home" lockdowns, most lasting multiple months. The policies of the regions with lower

ancies between the Pearson correlations of these two groups could be due to a variety of reasons, for example, differing camera distribution relative to population density, variations in camera resolution, and sporadic policies. These examples illustrate why a causal link cannot be established between policy changes and the current results. Nevertheless, the results demonstrate the real potential for computer vision methods on network camera data to provide a quantitative, meaningful, and coherent component for reasoning about the nuanced issue of observed human activities during pandemics. This method may be useful to epidemiologists modeling behaviors, policymakers improving future policies, and scientists conducting mobility

levels of correlation had consider-

ably fewer, shorter lockdowns, largely

favoring selective school and business

It is important to note that discrep-

closings instead.

research of any kind. We acknowledge that this study has some limitations. First, the observation presents correlations, not causation. Even though it would be convenient to claim that people responded to changes of policies, the reality can be far more complex. One noticeable factor is that in summer 2020, many places in the United States had protests for racial equality, and the large crowds were observed in the collected data. Second, this study aggregates different types of locations and does not consider seasonal factors. It is noticed that Austria has significantly high mobility at the beginning of 2021. A closer inspection discovers that many network cameras were deployed by ski resorts and thus showed many skiers.

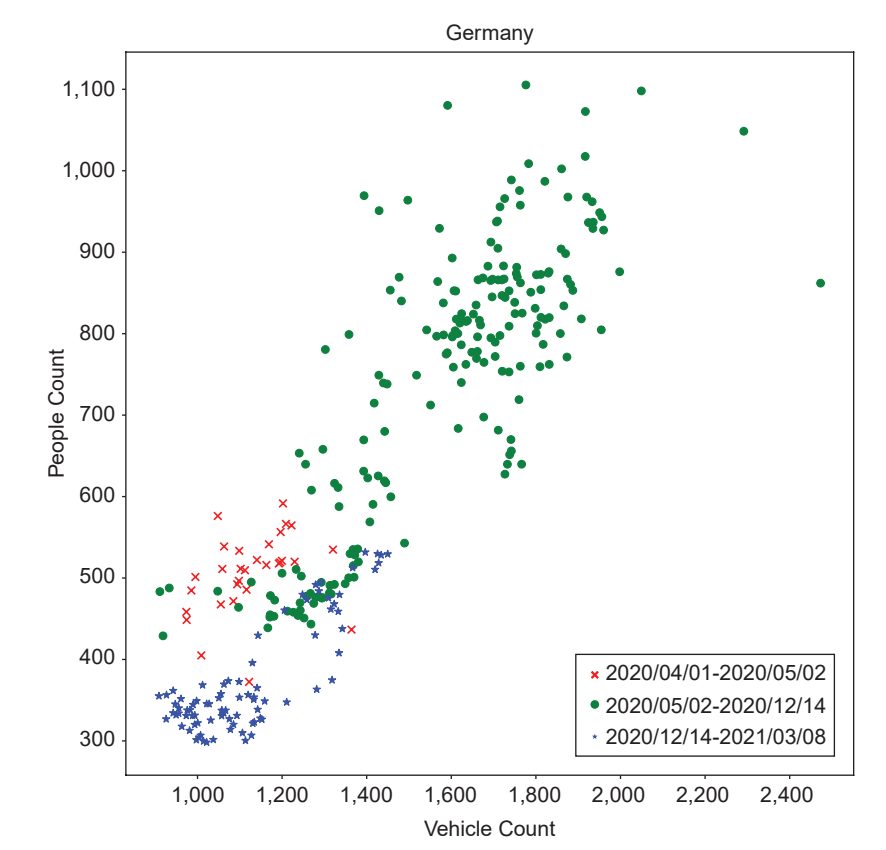


FIGURE 7. An example of a scatterplot of our data (Germany). The three groups of dates are divided by the large lockdown changes in Germany (the same as the graph markings in Figure 6). The scatterplot reveals three distinct clusters in the data that align with the date groups.

ABOUT THE AUTHORS

SHANE ALLCROFT is a research engineer in the BrainGate lab at Brown University, Providence, Rhode Island, 02912, USA. His research interests include brain computer, interfaces, computational neuroscience, computer vision, and machine learning. Allcroft received a B.S. in computer science from Purdue University. Contact him at shane@allcroft.net.

MOHAMMED METWALY is a graduate research assistant at Purdue University, West Lafayette, Indiana, 47907-2035, USA. His research interests include machine learning, computer vision, and wireless communication. Metwaly received a B.S. in computer engineering from Purdue University. Contact him at mmetwaly@purdue.edu.

ZACHERY BERG is a computer vision algorithm researcher at Zebra Technologies, Lincolnshire, Illinois, 60069, USA. His research interests include computer vision and reinforcement learning. Berg received a master's in computer science from Purdue University. Contact him at bergz1998@gmail.com.

ISHA GHODGAONKAR is a machine learning engineer at MITRE, San Diego, California, 92106, USA. Her research interests include computer vision, natural language processing, and related domains. Ghodgaonkar received a B.S. in computer engineering from Purdue University. Contact her at ighodgao@purdue.edu.

FISCHER BORDWELL is a graduate research assistant at Purdue University, West Lafayette, Indiana, 47907-2035, USA, who is interested in computer vision. His research interests include machine learning and reducing bias in machine learning. Bordwell received a B.S. in computer engineering from Purdue University. Contact him at fbordwel@purdue.edu.

XINXIN ZHAO is a master's student of computer science at Columbia University, New York City, New York, 10027, USA. Her research interests include computer science, data analytics, analytics, and data analysis. Zhao received a B.S. in computer science and data science from Purdue University. Contact her at xz3061@columbia.edu.

XINGLEI LIU is a master's student of applied data science at the University of Southern California, Los Angeles, California, 90089, USA. Her research interests include data science, machine learning, and computer vision. Liu received a B.S. in computer science from Purdue University. Contact her at xingleil@usc.edu.

JIAHAO XU is a silicon design engineer at AMD, West Lafayette, Indiana, 47906, USA. Xu received a B.S. in computer

engineering from Purdue University. Contact her at amyjxu@outlook.com.

SUBHANKAR CHAKRABORTY is a quantitative researcher at Graviton Research Capital, Gurgaon, Haryana, 122002, India. His research interests include computer vision, machine learning, statistics, and probability theory. Chakraborty received a B.S. in electrical and electronics engineering from the Indian Institute of Technology Madras. Contact him at subhankarchakraborty415@gmail.com.

VISHNU BANNA is a machine learning engineer at Apple, San Francisco, California, 94108, USA. His research interests include deep learning, computer vision, and robotics. Banna received a B.S. in computer engineering from Purdue University. Contact him at banna3vishnu@gmail.com.

AKHIL CHINNAKOTLA works in software engineering at Capital One, New York City, New York, 10011, USA. His research interests include computer vision, financial technology, and smart home devices. Chinnakotla received a B.S. in computer engineering from Purdue University. Contact him at achinnak@purdue.edu.

ABHINAV GOEL is a senior deep learning architect at NVIDIA, Santa Clara, California, 95051, USA. His research interests include machine learning systems. Goel received a Ph.D. from Purdue University. This work was conducted when Goel was at Purdue University. Contact him at goel39@ purdue.edu.

CALEB TUNG is a Ph.D. candidate at Purdue University, West Lafayette, Indiana, 47907-2035, USA, who is researching low-power computer vision. His research interests include computer vision and low-power machine learning. Tung received a B.S. in computer engineering from Purdue University. Contact him at tung3@purdue.edu.

GORE KAO is a master's student studying electrical and computer engineering at Carnegie Mellon University, Pittsburgh, Pennsylvania, 15213, USA. His research interests include machine learning, computer vision, image processing, and artificial intelligence. Kao received a bachelor's degree in electrical engineering from Purdue University. Contact him at gorek@andrew.cmu.edu.

WEI ZAKHAROV is an associate professor of library science and engineering information specialist in the Purdue University Libraries and School of Information Studies, West Lafayette, Indiana, 47907-2035, USA. Her research

interests include online-learning and data literacy education. Zakharov received a Ph.D. from Purdue University. Contact her at zakharov@purdue.edu.

DAVID A. SHOHAM is a professor of biostatistics and epidemiology and the department chairperson in the College of Public Health, East Tennessee State University, Johnson City, Tennessee, 37615, USA. His research interests include chronic disease epidemiology and social network analysis. Contact him at shoham@etsu.edu.

GEORGE K. THIRUVATHUKAL is a professor of computer science and the department chairperson at Loyola University Chicago, Chicago, Illinois, USA. His research interests

include high-performance computing, languages and systems, distributed systems and clouds, and machine Learning and computer vision. Thiruvathukal received a Ph.D. from Illinois Institute of Technology. He is also a visiting computer scientist at the Argonne National Laboratory in the Leadership Computing Facility. Contact him at gthiruvathukal@luc.

YUNG-HSIANG LU is a professor of electrical and computer engineering and a university faculty scholar at Purdue University, West Lafayette, Indiana, 47907-2035, USA. His research interests include computer vision, embedded systems, and cloud computing. Lu received a Ph.D. from Stanford University. Contact him at yunglu@purdue.edu.

This study counts the numbers of people and vehicles and does not identify any individuals (for example, it does not recognize faces or license plates). The images used in this study do not have enough pixels for identification (please see Figures 1 and 4 as examples). This study has been approved by the Institutional Review Board of Purdue University.

his article presents a method using computer vision to quantify mobility during the COVID-19 pandemic. This study counts the number of people and vehicles using data from public network cameras across five countries and three U.S. states. The method produces mobility trends that agree with the timeline of policy changes. In the future, analyzing visual data could be used to corroborate other mobilization sources (such as cell phone mobilization data sets and public policy data sets) and could be used as evidence to craft effective policy in any future events.

At the time of writing, there is every reason to believe that this will not be the last pandemic as contagious variants continue to spread across the world. The future will likely have even greater network camera coverage as deployments continue apace throughout the world, especially in major urban areas. The techniques presented here show a strong potential for aiding in the observation and analysis of human response to future pandemics, and at a minimum, there is a strong case to include computer vision in the toolbox for future public health and policy purposes.

ACKNOWLEDGMENTS

This study is supported in part by NSF OAC-2027524. This research uses resources of the Argonne Leadership Computing Facility, which is a U.S. Department of Energy Office of Science User Facility supported under Contract DE-AC02-06CH11357. We thank the Argonne Leadership Computing Facility for access to the Cooley supercomputer and Eagle large-scale storage resources that were used in this study. The views and opinions in this article are those of the authors and do not necessarily represent the views of the sponsors. Shane Allcroft and Mohammed Metwaly contributed equally to this work.

REFERENCES

- J. Ma, "China's first confirmed COVID-19 case traced back to November 17," South China Morning Post, Mar. 13, 2020. [Online]. Available: https://www.scmp.com/news/ china/society/article/3074991/ coronavirus-chinas-first-confirmed -covid-19-case-traced-back
- S. Nebehay, "WHO says new China coronavirus could spread, warns hospitals worldwide," Reuters, Jan. 14, 2020. [Online]. Available: https:// www.reuters.com/article/us -china-health-pneumonia-who -idUSKBN1ZD16J
- 3. R. Saavedra, "Global emergency declared over coronavirus, first Transmission Confirmed in U.S.," The Daily Wire, Jan. 30, 2020.
- 4. R. Dailey et al., "Automated discovery of network cameras in heterogeneous web pages," ACM Trans. Internet Technol., vol. 22, no. 1, pp. 1–25, doi: 10.1145/3450629.
- T. Hale et al., "A global panel database of pandemic policies (Oxford COVID-19 government response tracker)," Nature Human Behav., vol. 5, no. 4, pp. 1–10, 2021, doi: 10.1038/ s41562-021-01079-8.

- 6. "COVID-19 community mobility report," Google. https://www.google.com/covid19/mobility/
- "Mobility trends reports," Apple.
 [Online]. Available: https://covid19.
 apple.com/mobility
- 8. C. Chapin and S. S. Roy, "A spatial web application to explore the interactions between human mobility, government policies, and COVID-19 cases," *J. Geovis. Spatial Anal.*, vol. 5, no. 1, p. 12, 2021, doi: 10.1007/s41651-021-00081-y.
- 9. I. Hasan, S. Liao, J. Li, S. U. Akram, and L. Shao, "Generalizable pedestrian detection: The elephant in the

- room," in Proc. IEEE/CVF Conf. Comput. Vis. Pattern Recognit. (CVPR), Jun. 2021, pp. 11,328–11,337.
- B. Zhou, A. Lapedriza, A. Khosla, A.
 Oliva, and A. Torralba, "Places: A 10
 million image database for scene
 recognition," *IEEE Trans. Pattern Anal.* Mach. Intell., vol. 40, no. 6, pp. 1452–
 1464, 2017, doi: 10.1109/TPAMI.2017.
 2723009.
- 11. S. Shao et al., "Crowdhuman: A benchmark for detecting human in a crowd," 2018, arXiv:1805. 00123.
- 12. Z. Cai and N. Vasconcelos, "Cascade R-CNN: High quality object detection

- and instance segmentation," 2019, arXiv:1906.09756.
- R. Girshick, I. Radosavovic, G. Gkioxari, P. Dollár, and K. He, "Detectron," GitHub, San Francisco, CA, 2018. [Online]. Available: https://github.com/facebookresearch/detectron
- 14. T.-Y. Lin et al., "Microsoft COCO: Common objects in context," in Proc. Eur. Conf. Comput. Vis., 2014, pp. 740–755.
- Y.-H. Lu et al., "See the world through network cameras," Computer, vol.
 no. 10, pp. 30–40, Oct. 2019, doi: 10.1109/MC.2019.2906841.



Digital Object Identifier 10.1109/MC.2023.3241499